Geophys. J. Int. (2007) **169,** 941–950 doi: 10.1111/j.1365-246X.2007.03378.x

Oceanic basalt continuous thermal demagnetization curves

Jürgen Matzka[1,*] and David Krása[2]

[1]*Earth and Environmental Sciences, Ludwig-Maximilians-Universität München, Theresienstr.* 41 80333, *Munich, Germany*
[2]*School of GeoSciences, University of Edinburgh, Edinburgh* EH9 3JW, *UK. E-mail: david.krasa@ed.ac.uk*

Accepted 2007 January 17. Received 2007 January 17; in original form 2006 August 25

SUMMARY

The palaeomagnetic standard technique of stepwise thermal demagnetization (STD), long regarded as unreliable for oceanic basalts that have undergone low temperature alteration, has recently been applied in a number of studies to characterize the natural remanent magnetization (NRM) of such rocks. In order to better understand STD data of oceanic basalts, and to possibly identify the magnetominerals that are carrying the NRM, we have carried out a number of continuous and STD experiments on seven oceanic basalt samples. During continuous thermal demagnetization (CTD), a sample is heated to a certain temperature and its NRM is measured during heating and subsequent cooling. Even when CTD reveals only titanomaghemite unblocking at 400°C as the remanence carrier, STD behaviour can be very complex and unblocking is observed at temperatures of up to 500°C and higher. CTD also allowed to identify a partial or full self-reversal of NRM due to interaction between two types of magnetominerals in one sample. The higher degree of maghemitization of smaller titanomaghemite grains with respect to larger ones, which are less efficient in carrying the remanence, was seen for three samples by a shift of 80°C between the strong field thermomagnetic curve and the NRM measured at elevated temperature. In several cases, the identification of the NRM-carrying magnetomineral was not possible from CTD data due to the ambiguity of Curie temperatures in the titanomagnetite/titanomaghemite system.

Key words: demagnetization, ocean drilling program, oceanic crust, palaeomagnetism, rock magnetism, titanomagnetite.

1 INTRODUCTION

Unblocking temperatures of the natural remanent magnetization (NRM) of oceanic basalts determined by stepwise thermal demagnetization (STD) are often higher than their Curie temperatures from strong field measurements. STD data of oceanic basalts was long regarded as prone to artefacts and difficult to interpret due to the thermal instability of the remanence-carrying minerals (Irving 1970) and seldom used in subsequent studies (e.g. Kent and Gee 1994). However, in several recent publications (Kent & Gee 1994; Kent & Gee 1996; Zhou *et al.* 1999; Doubrovine & Tarduno 2004; Doubrovine & Tarduno, 2005; Wang *et al.* 2005; Doubrovine & Tarduno 2006), STD data of oceanic basalts has played an important role for the identification of the remanence-carrying minerals and the alteration they undergo as well as for studying causes of the long term trend in NRM intensity of oceanic basalts and of partial or complete self-reversal of the NRM. Low field thermomagnetic heating curves resembling continuous thermal demagnetization (CTD, measurement of NRM at elevated temperature T) data of oceanic basalts have been reported by Johnson & Tivey (1995) and Zhou *et al.* (1999) and CTD data from both heating and cooling in zero field were reported by Matzka *et al.* (2003) and more recently by Krása & Matzka (2007). In the present paper we describe a series of CTD experiments on oceanic basalts that show features that are invisible in STD. Nevertheless, CTD also has its diagnostic limits in elucidating the origin and the processes affecting the NRM and its carriers and the limited sample set studied with this method does not yet allow to draw general conclusions. However, CTD experiments allow a better understanding of the existing STD data of oceanic basalts and show where further systematic CTD studies can lead. We will first describe the typical model of oceanic basalt magnetomineralogy (following Petersen *et al.* 1979 and references therein) and its limitations and then discuss the results of previous STD and CTD studies.

A simple description of oceanic basalt magnetomineralogy starts with a primary titanomagnetite $Fe_{3-x}Ti_xO_4$ with $x \approx 0.6$ (also known as TM60) with some minor other cations (e.g. Al, Mg) crystallizing in the cooling lava. The high cooling rate of the sea water quenched magma inhibits deuteric oxidation (typically occurring at temperatures above 300°C) to a low-Ti titanomagnetite. At seafloor conditions, the TM60 is still prone to oxidation and affected by the so-called low temperature oxidation or maghemitization. This process maintains the inverse spinel lattice and the charge balance

*Current address: Danish Meteorological Institute, Lyngbyvei 100, DK-2100 Copenhagen, Denmark, E-mail: jmz@dmi.dk

but reduces the number of Fe^{2+} by removal of Fe ions and oxidation of remaining Fe^{2+} to Fe^{3+}. The resulting Fe depleted mineral is called titanomaghemite (in this text frequently referred to as maghemitized TM60) and the degree of maghemitization is described by the ratio z of transformed Fe^{2+} to originally present Fe^{2+}. Maghemitization is a slow process and accompanied by changes in the magnetic properties like the temperature dependence of spontaneous magnetization $M_S(T)$ and the Curie temperature T_C (Readman & O'Reilly 1972). Zhou *et al.* (2001) found z to be limited to 0.35 for Quaternary (<2 Ma) samples and $z < 0.8$ for 2–10 Ma old samples, maximum reported values were $z = 0.92$. According to Ryall & Ade-Hall (1975a), inversion of titanomaghemites is not observed at seafloor conditions but starts from 100°C onwards. Although there are several accounts of highly maghemitized TM60 inverting under seafloor conditions to various oxides (e.g. Petersen 1976) and of the possibility of remanence inheritance during this process (Kent & Gee 1994), this still seems to be an open question in the literature. At temperatures above 300°C titanomaghemite inversion is well studied and results in low-Ti titanomagnetite (e.g. Özdemir 1987).

This simple model of oceanic basalt magnetomineralogy is complicated in nature by strong gradients in magnetic properties within single pillows (e.g. Ryall & Ade-Hall 1975b) as well as in massive flows that can arise either from differences in the primary magnetominerals or differences in the influence of maghemitization. Single-domain titanomagnetite with a great compositional variation from TM00 to TM80 has been observed in the glassy matrix of otherwise TM60 bearing oceanic basalts (Zhou *et al.* 1997). An extreme case is fine-grained TM60 embedded in interstitial glass that are protected from low temperature oxidation over tens of millions of years (Zhou *et al.* 1999, 2001).

Kent & Gee (1994) and Kent & Gee (1996) identified two magnetic phases from STD that are carrying NRM in young oceanic basalt. One is an ensemble of maghemitized TM60 grains where the preferentially oxidized smaller grain sizes are very efficient NRM carriers (Bina & Prevot 1989) with an unblocking temperature around 300°C and where the less oxidized larger and volumetrically more important grain sizes account for a Curie temperature below 200°C. The other phase is recognized from unblocking of a very small proportion of NRM at temperatures typical for low-Ti titanomagnetite. The most likely explanation was that the low-Ti titanomagnetite and its remanence originated from inversion of maghemitized TM60 or that it was present as a primary magmatic phase. A formation of low-Ti titanomagnetite during laboratory heating was thought to be unlikely. However, by employing microanalytical methods, Zhou *et al.* (1997) have identified titanomagnetites with a broad range of x values in these samples that can well explain the unblocking at 300°C and at the magnetite Curie temperature around 575°C. Zhou *et al.* (1999) also identified titanomagnetites that were protected from oxidation in interstitial glass of >10 Ma old samples and showed that the NRM of ODP sample 556–4R–3(80–90) (sample code following ODP nomenclature) has unblocking temperatures typical for this titanomagnetite both in STD and CTD that are well below the Curie temperature of 310°C typical for maghemitized TM60.

Doubrovine & Tarduno (2004) and Doubrovine & Tarduno (2005) observed a self-reversal of magnetization for seamount basalts containing titanomaghemites with $0.65 < x < 0.85$ and $z > 0.95$. STD data isolated a normal NRM component at unblocking temperatures above 300°C to 400°C and an antiparallel self-reversed component which crossed the origin during stepwise demagnetization below 300°C to 400°C. Samples containing two antiparallel components but not crossing the origin during isolation of the low temperature component (in this case the low temperature component has lower intensity than the high temperature component) were interpreted to have undergone partial self-reversal. Although magnetic interaction could not be excluded as the responsible mechanism, experimental evidence pointed towards Nèel N-type self-reversal due to ionic ordering as the more likely underlying mechanism (Doubrovine & Tarduno 2004). Another study involving STD of oceanic basalts by Wang *et al.* (2005) isolated a weak antiparallel NRM component at temperatures up to 300°C that qualitatively resembles the partially self-reversed samples by Doubrovine & Tarduno (2004). Wang *et al.* (2005), however, interpret that feature as a magnetic overprint and conclude that this overprint can not be responsible for long term NRM intensity trends.

In a previous study, Matzka *et al.* (2003) have argued that titanomaghemite ($x \approx 0.6$ and $z \approx 0.8$) with $M_S(T)$ curves of Nèel N- or P-type with a maximum above room temperature are typical for approximately 10–40 Ma old oceanic basalts containing maghemitized TM60. CTD curves from room temperature to 600°C and back have been shown for four samples (470A–8–3(27–29), 79–17–1(102–104), 556–4–3(30–32), 556–5–2(73–75)) to demonstrate that the NRM displays a maximum above room temperature due to its $M_S(T)$-curve type and that consequently the titanomaghemite is the predominant remanence carrier.

2 SAMPLES AND TECHNIQUES

The samples are oceanic basalts recovered by DSDP/ODP. The specimens do not contain glassy rims. Their samples' code, age, ocean of origin, and the magnetic parameters T_C, saturation remanence over saturation magnetization M_{RS}/M_S, coercive force H_C, coercivity of remanence H_{CR}, and M_S are given in Table 1 and correspond to the data already published in Matzka *et al.* (2003). Rock magnetic measurements were conducted on a 4 mm diameter subsample with a VFTB (maximum field strength of 0.63 T), leading to an underestimation of M_S and an overestimation of M_{RS}/M_S for the magnetically most stable samples. Thermomagnetic curves as a proxy to $M_S(T)$-curves are displayed in the upper panels of Figs 1(a)–(f). They were measured in a field of 0.4 T and are shown before (upper curve) and after (lower curve) correction for the paramagnetic contribution. The paramagnetic magnetization was determined at room temperature from hysteresis loops and a reciprocal dependency on absolute temperature and a linear dependency on the external magnetic field was assumed. For magnetically stable oceanic basalts, the paramagnetic contribution determined from not fully saturated hysteresis loops could be slightly overestimated (Matzka *et al.* 2003) and then the upper and lower curves in the upper panel of Figs 1(a)–(f) give the upper and lower limit of the $M_S(T)$-curve.

The CTD data of a NRM-carrying sample is now referred to as $NRM(T)$. The $NRM(T)$ presented in Fig. 1 for each of the above mentioned oceanic basalts was measured for two differently oriented sister samples with a self-assembled spinner magnetometer (HOTSPIN I) with integrated oven at the palaeomagnetic laboratory of the University Munich. $NRM(T)$ is the NRM measured at (elevated) temperature T. HOTSPIN I reaches a maximum temperature of 600°C. Its sensitivity is estimated to 5×10^{-8} Am^2/kg. There is no sample manipulation except spinning during CTD and consequently only magnetization components in the plane perpendicular to the axis of rotation are measured. In Fig. 1, the absolute value of intensity normalized to 1 and the phase of the spinner signal is given for two perpendicular planes, labelled the X-Z and the

Table 1. Sample description and magnetic properties.

ODP sample code	Age [Ma]	Ocean	T_C [°C]	T_m [°C]	M_{RS}/M_S *	H_C [mT]	H_{CR} [mT]	M_S [Am^2/kg]
507B-1-1(56–58)	0.7	Pacif.	145	–	0.208	7.6	14.1	0.992
157-49-2(131–133)	8	Pacif.	250	–	0.117	4.6	8.8	1.282
470A-9-2(49–51)	15.7	Pacif.	325	130	0.431	17.1	21.4	0.236
556-5-2(73–75)	32	Atl.	305	175	0.770	52.9	65.0	0.046
77B-54-1(18–20)	36	Pacif.	320	115	0.562	27.2	38.1	0.301
170-16-2(19–21)	100	Pacif.	295/530	–	0.130	6.9	13.4	0.958
550B-29-1(30–32)	102	Atl.	295	–	0.183	6.2	11.5	0.995

T_m: temperature of maximum in $M_S(T)$ when occurring above room temperature after subtraction of paramagnetic component from thermomagnetic curve.
Magnetic parameters: Curie temperature T_C, saturation remanence per saturation magnetization M_{RS}/M_S, coercive force H_C, coercivity of remanence H_{CR}, saturation magnetization M_S.
*Reported values are from measurements in maximum fields of 0.63 T (*cf.* Matzka *et al.* 2003)

Y-*Z* plane. The heating and cooling curves of $NRM(T)$ intensity are shown as lines in the same panel, the heating curves being those starting at intensity 1. For the $NRM(T)$ phase, the heating (crosses) and cooling curves (diamonds) are shown in two separate panels. For most samples the NRM direction within the measurement plane (labelled *X*-*Z* plane in Fig. 1) did not change, suggesting directionally stable magnetization components that were confirmed with measurements on sister samples rotated by 90° (labelled *Y*-*Z* plane in Fig. 1), except for sample 157–49–2(131–133) (see Fig. 3). However, overlapping directional magnetization components are more difficult to isolate during CTD than during STD (Schmidt & Clark, 1985). The instrument is efficiently shielded against external fields by mu-metal (as can be seen from zero intensity and random phase at cooling of $NRM(T)$ after full demagnetization, e.g. Figs 1(d) and (e)), For samples 556–5–2(73–75) and 157–49–2(131–133) a STD was performed on a 9 mm subsample with a Schoenstedt oven and the 2G cryogenic magnetometer at the palaeomagnetic laboratory of the University Munich.

In the following text, the samples from Table 1 one will be referred to by their DSDP/ODP code site number only, samples from other studies by their complete ODP sample code. The samples will be presented in the order of their age, with exception of 157 that showed a special behaviour and will be treated last.

3 RESULTS

The thermomagnetic curves of samples 507B, 470A, 77B and 556 are shown in the upper panel in Figs 1(a)–(d) and the Curie temperatures are given in Table 1. The lowest Curie temperature (145°C, sample 507B) is typical for TM60 (e.g. Dunlop & Özdemir 1997). The Curie temperatures between 305°C and 325°C of the other three samples are typical for maghemitized TM60. The presence of maghemitized TM60 is confirmed by the maximum in $M_S(T)$ above room temperature (for 77B and 556 only visible after paramagnetic correction; the maximum in $M_S(T)$ for 556 was already confirmed in Matzka *et al.* 2003). Samples 470A and 77B display a second maximum in the thermomagnetic curve around 480°C. This magnetic phase typically is a titanomagnetite (T_C around 550°C) with low Ti content ($x \approx 0.1$ or TM10) formed during heating as inversion product of maghemitized TM60 (e.g. Özdemir 1987). The maximum in $M_S(T)$ indicates that this phase was formed during the laboratory heating, but magnetization does not completely disappear between the maghemitized TM60 and the TM10 (especially for 470A) and it can not be excluded that there already exists a TM10 or a phase with a similar Curie temperature in the unheated sample. For sample 556, the maximum in $M_S(T)$ around 530°C is clearly the result of the inversion of maghemitized TM60 during laboratory heating.

The $NRM(T)$ heating curves in the lower panels of Figs 1(a)–(d) show a major decrease in NRM intensity and no directional change (crosses) corresponding to the TM60 and maghemitized TM60 phase. The NRM decrease of these phases is characterized by an almost linear decay (e.g. for 507B around 200°C) followed by a concave part (between 220°C and 280°C for 507B). The concave part of the curve occurs for samples 507B, 77B and 556 at temperatures significantly above the Curie-temperatures and the temperature at which $NRM(T)$ decreases to 50% of its initial value is approximately 80°C higher than the temperature at which $M_S(T)$ decreases to 50%. Following Bina & Prevot (1989), this discrepancy could best be explained by a higher oxidation degree and therefore higher Curie temperature of the smaller grains of the maghemitized TM60 phase. In fact, microprobe analysis of sample 507B reveals an increasing maghemitization degree from larger (60 micron) to smaller (15 micron) grains by $z \approx 0.3$ (fig. 3.18 in Matzka 2001). Maghemitized TM60 as NRM carrier is also confirmed by the presence of a maximum in $NRM(T)$ above room temperature, which is well developed for sample 556 (see also Matzka *et al.* 2003) and also observable in the *Y*-*Z* plane of 77B (Fig. 1c). Sample 507B has a $NRM(T)$ intensity heating curve without a maximum above room temperature, which is compatible with the low age and oxidation degree. For samples 507B a TM60 and for 77B and 556 a maghemitized TM60 magnetomineralogy with a slightly higher mean oxidation degree z of the remanence-carrying particles could well explain the data in Fig. 1. A difference in z of 0.25 would approximately lead to an 80°C higher Curie temperature (Readman & O'Reilly 1972).

Sample 470 A is different. The $NRM(T)$ intensity has no maximum above room temperature and two clearly distinct unblocking temperatures can be observed. The first unblocking is in the same temperature range as the $M_S(T)$ curve and there is no temperature shift by approximately 80°C as for the samples discussed before. Due to the lack of NRM properties typical for maghemitized TM60, titanomagnetite with T_C around 350°C (TM35) might be the NRM carrier. The second unblocking occurs around 520°C and a composition of the NRM carrier around TM10 is very likely, accounting for 10–20% of the original NRM. Both titanomagnetite compositions lie within the range observed for single-domain (and therefore efficient) remanence carriers observed in interstitial glass of ocean basalts (Zhou *et al.* 1997). This would suggest a magmatic origin of the remanence carriers.

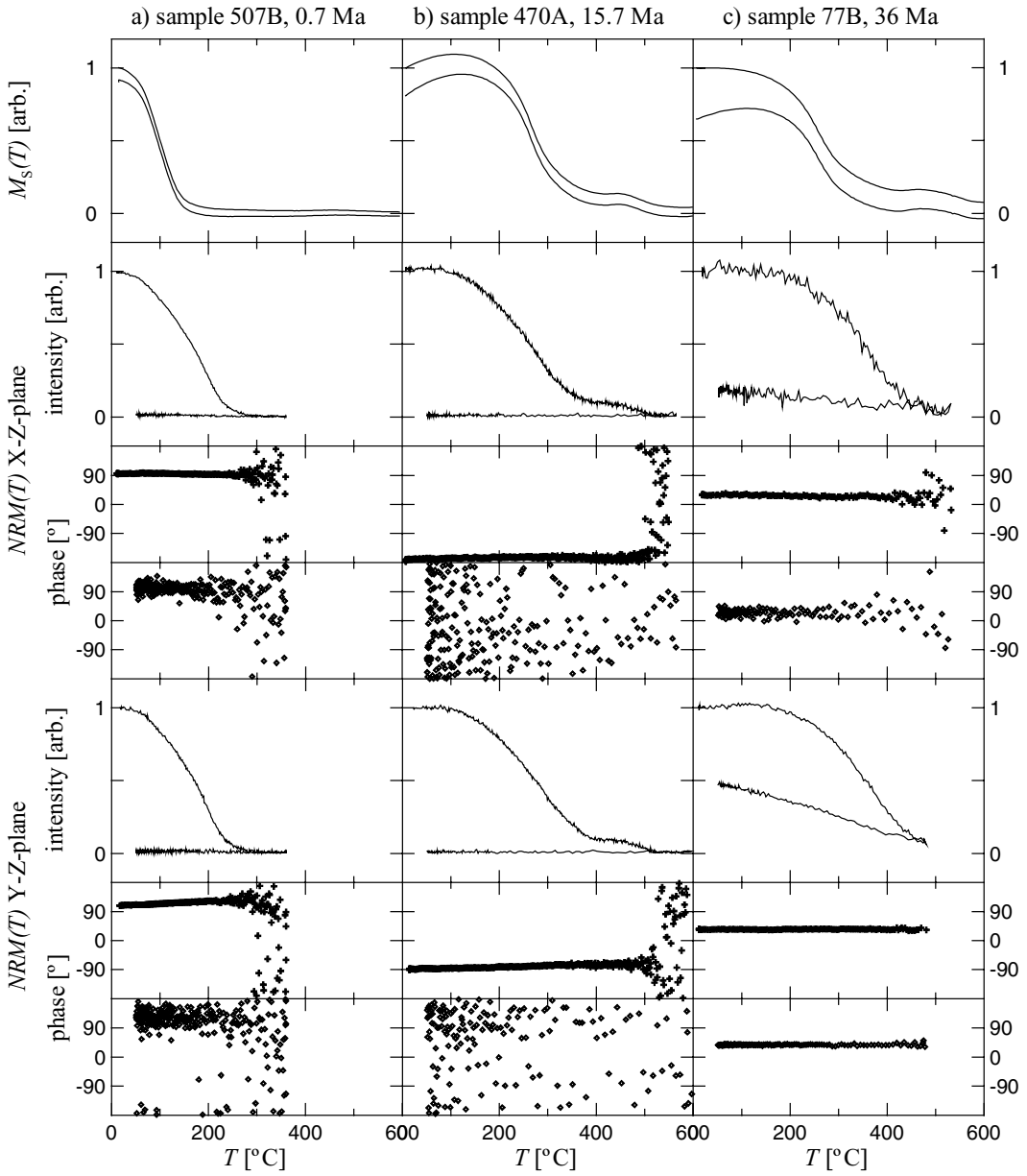

Figure 1. Comparison of strong field thermomagnetic curves $M_S(T)$ with continuous thermal demagnetization $NRM(T)$ of NRM for oceanic basalt samples 507B (a), 470A (b), 77B (c), 556 (d), 170 (e) and 550B (f). For $M_S(T)$ a strong field thermomagnetic curve is given before (upper curve) and after (lower curve) correction for paramagnetism. $NRM(T)$ is given for two perpendicular measurement planes (X-Z, Y-Z). All magnetizations in arbitrary units, the phase information (direction of magnetization within core coordinate X-Z or Y-Z-plane) is for arbitrary zero position. The phase information for a single $NRM(T)$ curve is given in separate panels for the heating (crosses) and the cooling (diamonds) curve.

The $NRM(T)$ cooling curves depend on the maximum temperature of the heating run, and different phenomena can be observed in Figs 1(a)–(d). Sample 556 in Fig. 1(d) was heated to 600°C in the X-Z plane and the directional information (phase of the spinner signal, crosses) starts to become random at about 400°C where the intensity drops below the sensitivity level during heating and remains random during cooling (diamonds). This clearly demonstrates that no measurable remanences were acquired in the instrument during cooling. The shape of the curve also suggests that the maghemitized TM60 fully demagnetizes at 400°C. There is no indication of inheritance of magnetic remanence during the inversion of the maghemitized TM60 from the mother to the daughter phase, either because the remanence of the daughter phase is too small to be measured between 400°C and its unblocking, or because the mother phase NRM is fully demagnetized at 400°C, below the onset of inversion that can be monitored in the $M_S(T)$ curve to happen around 450°C. The $NRM(T)$ curve in the Y-Z plane has a maximum temperature of 460°C, and although the remanence falls below the sensitivity of the instrument at around 400°C, a remanence in the same direction recovers during cooling between 400°C and room temperature to 25% of its original value. The shape of the $NRM(T)$ intensity during cooling suggests a kink around 400°C, being below sensitivity above and linearly increasing below that temperature. In any case, during STD the final unblocking would have been assumed to be above 460°C as will be discussed below.

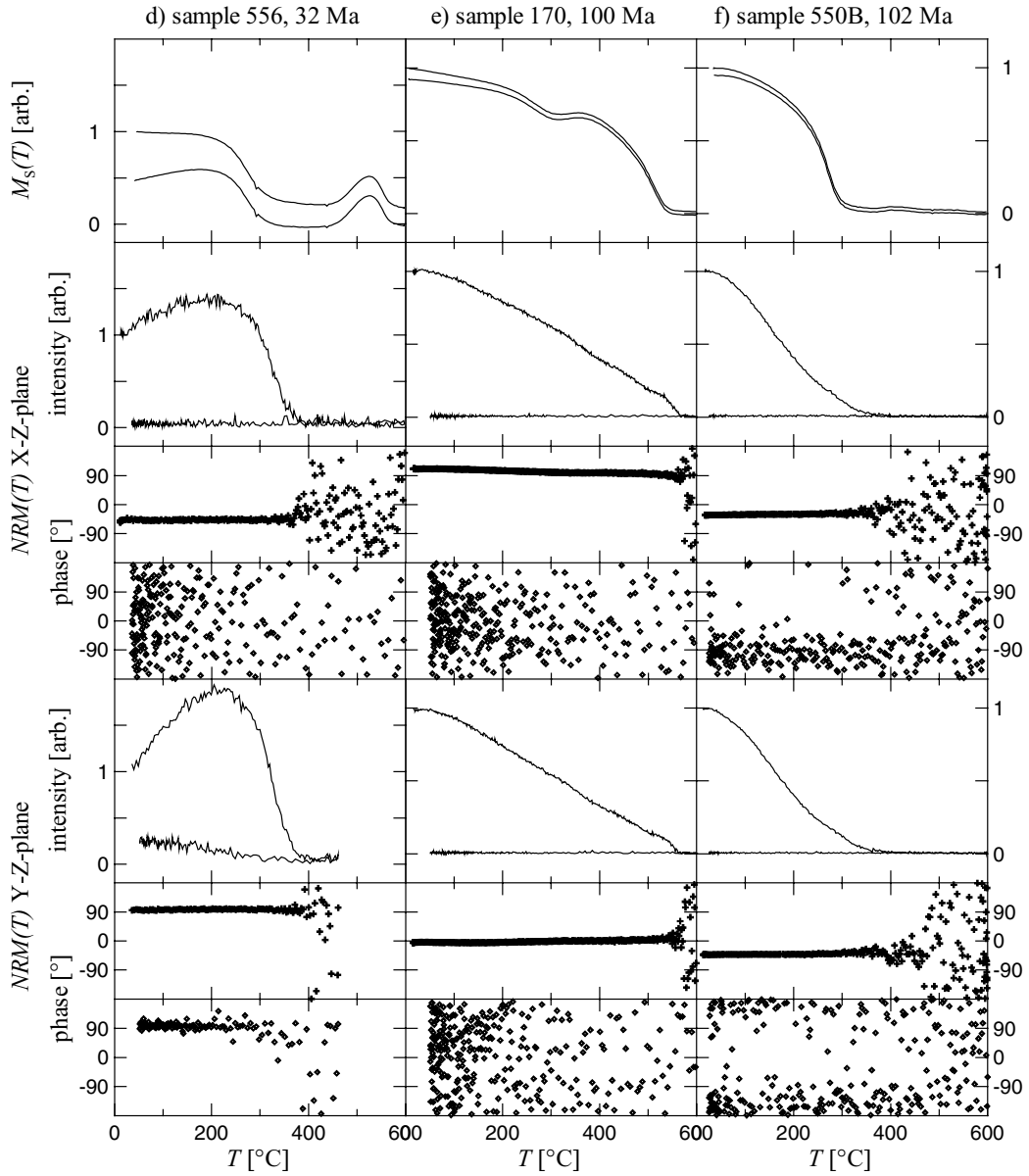

Figure 1. (*Continued*.)

For the two CTD experiments on sample 77B in Fig. 1(c), the maximum temperatures are 480°C (*Y*-*Z* plane) and 520°C (*X*-*Z* plane), which is well above the Curie temperature of 320°C, and the *NRM*(*T*) cooling curves show a remaining remanence at room temperature that amounts to 45% and 15%, respectively, of the intensity in the original NRM direction. Plotting this remaining remanence in the style of STD decay curves, a remanence carrier with composition close to magnetite would be assumed. The shape of the cooling curve resembles a linear segment without a kink and gives no indication about the inversion process of the maghemitized TM60, although it might play a role here since the maximum temperatures are within the temperature range of the formation of TM10 ($M_S(T)$ curve in Fig. 1c).

Above 300°C *NRM*(*T*) intensity of sample 507B becomes very small compared to the original NRM and a random *NRM*(*T*) phase between 300°C and the maximum temperature of 360°C indicate that the NRM intensity fell below the sensitivity level of the instrument. During cooling, a very small but directionally stable remanence in the original direction is observed, but this phase seems to gain intensity above the sensitivity level of the instrument only after cooling below 300°C to 250°C (the *NRM*(*T*) phase is becoming less scattered), whereas the unblocking temperature is above the maximum heating temperature of 360°C. Such behaviour would indicate an interaction between a high-T_C (>360°) and a low-T_C (around 250°C) phase.

The *NRM*(*T*) cooling curve of 470A (Fig. 1b) shows no gain of remanence during cooling from 565°C in the *X*-*Z* plane, but there is a preferred remanence orientation during cooling from 600°C in the *Y*-*Z* plane as indicated by the limited scatter of the phase (diamonds). However, this is directionally independent of the original remanence and might be a measurement artefact similar to those observed in STD experiments, where a remaining, directionally unstable remanence is observed after demagnetization.

A sister sample of 556 with the clear indication for maghemitized TM60 as remanence carrier (Fig. 1d) was additionally treated by STD (Figs 2a–c). STD is not able to identify the Néel

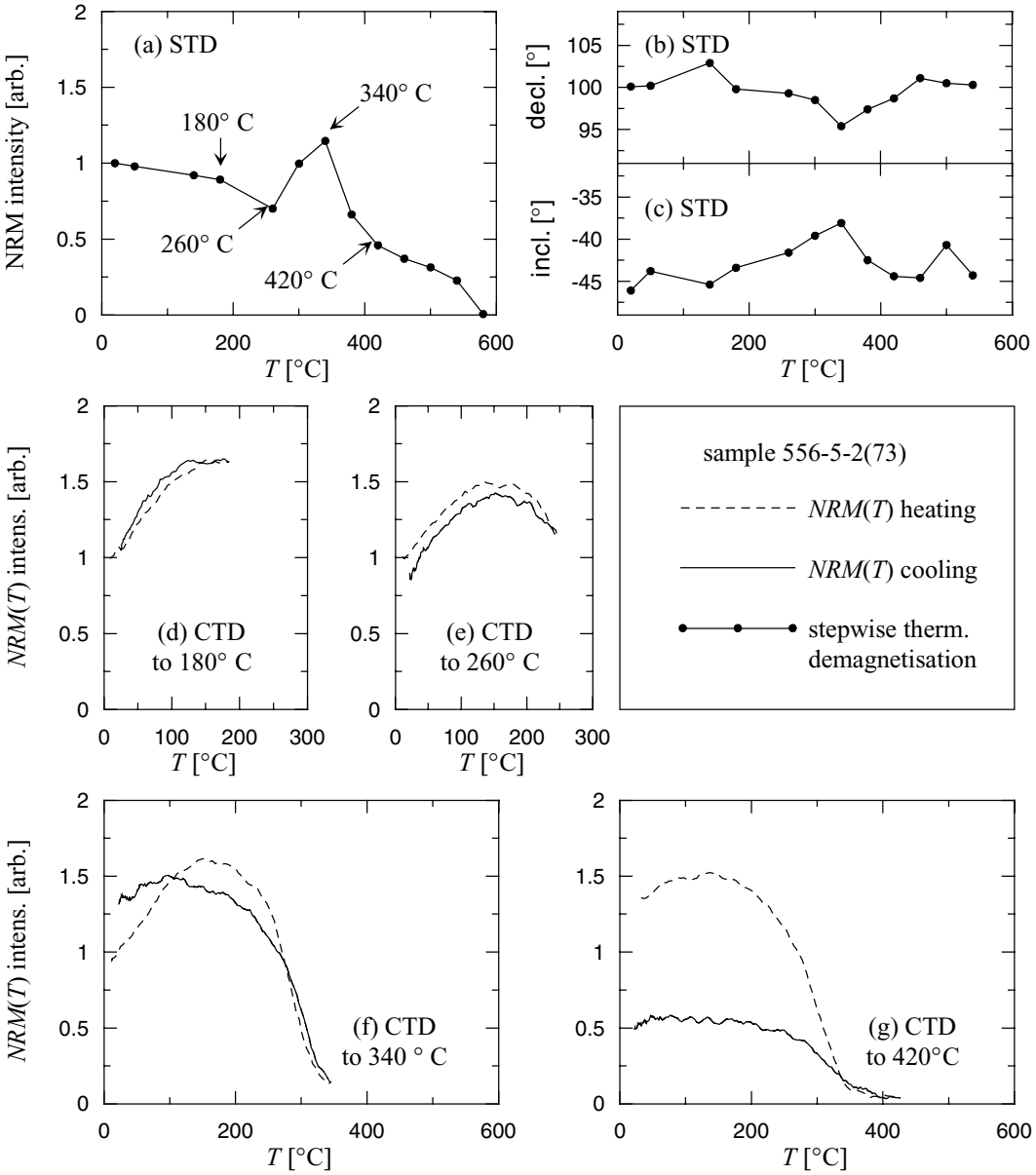

Figure 2. Stepwise (STD) and continuous (CTD) thermal demagnetization of sample 556. Intensity (a) and directional (b, c) information from STD. The CTD experiments in (d)–(g) with *NRM*(*T*) heating (dashed lines) and cooling (full lines) curves were performed to progressively higher maximum temperatures (also indicated by arrows in a).

P-type behaviour but reveals a complicated NRM intensity variation with a minimum after heating to 260°C and a maximum at 340°C (Fig. 2a) while the NRM direction remains constant (Figs 2b and c). The NRM is completely demagnetized between 540°C and 580°C. The STD steps with the temperature indicated in Fig. 2(a) where repeated in CTD on a fresh sister sample. Since a stable direction of NRM was expected from stepwise demagnetization, only the plane containing the full magnetization vector (the plane defined by the magnetization vector and the cylinder axis, which is perpendicular to the spinning axis) was measured with the HOTSPIN I instrument and the *NRM*(*T*) intensity curves are shown in Figs 2(d)–(g). The CTD shows no change in remanence direction within the measured plane up to 400°C when remanence directions become random (data not shown). An *NRM*(*T*) increase by more than 50% on heating to 180°C is reversible on cooling (Fig. 2d), confirming that the predominant remanence carrier is a titanomaghemite with typical Néel P- or N-type behaviour. The next continuous demagnetization cycle to 260°C clearly identifies the maximum above room temperature (Fig. 2e). The irreversible NRM intensity loss at room temperature of approximately 10%, attributed to remanence unblocking since at this low temperature no magnetomineralogical changes are expected, is slightly smaller than the approximately 20% loss observed during the corresponding STD (Fig. 2a). The next heating to 340°C results in an irreversible gain of remanence at room temperature by approximately 30% compared to the initial remanence before heating (Fig. 2f). However, at 340°C the remanence is diminished to approximately 20% of its initial value due to decreased spontaneous magnetization at this temperature. Since the *NRM*(*T*) cooling curve closely resembles the *NRM*(*T*) heating curve between 340°C and 280°C and even lies significantly below it between 280°C

and 100°C, the irreversible remanence gain at room temperature can not be due to unblocking of an antiparallel remanence component. However, inversion of titanomaghemite to Ti-poor titanomagnetite at or above 300°C would be a viable mechanism to explain this behaviour, if it allows for remanence being inherited from mother to daughter phase as proposed by Krása & Matzka (2007). The maximum in $NRM(T)$ is less pronounced in the $NRM(T)$ cooling curve and its temperature decreased from approximately 160°C to 100°C. This suggests that a part of the NRM is still carried by the maghemitized TM60 and a part is carried by the newly formed titanomagnetite. The increase in NRM at room temperature observed between 260°C and 340°C (Fig. 2a) might therefore be attributed to the inheritance of the NRM direction by the inversion product titanomagnetite, and the decrease in NRM at room temperature between 340°C and 420°C might be a combined effect of the unblocking (see Fig. 1d, $NRM(T)$ in the X-Z plane) and inversion of the maghemitized TM60 in this temperature interval. Although the $NRM(T)$ intensity is basically zero between 400°C and 420°C (Fig. 1d, X-Z and Y-Z plane, and Fig. 2g), on cooling, mainly between 400°C and 250°C, the intensity increases again to a value that is approximately 50 percent of the initial remanence (Fig. 2g). From STD of the sister sample we know that this remanence will only be fully demagnetized between 540°C and 580°C. CTD, however, shows that this high-temperature remanence is not carried by a primary low-Ti titanomagnetite that was present in this sample prior to heating and hence must be seen as an inversion product.

The 100 Ma old sample 170 has two Curie temperatures (Fig. 1e). The higher Curie temperature at 530°C belongs to a magnetic phase of which at least a part evidently is formed during heating (peak in $M_S(T)$ at 380°C). The $NRM(T)$ curve finally unblocks at 560°C, corresponding almost to magnetite, but exceeding the measured Curie temperature of 530°C (corresponding to TM10). In this case, it seems rather unlikely that the newly formed titanomagnetite is the remanence carrier by inheriting the NRM from the inverting maghemitized TM60 during heating. The NRM-carrying magnetite should therefore be of magmatic origin or a inversion product of maghemitized TM60 at seafloor conditions. The lower Curie temperature was determined to be 295°C but could be higher since the new formation of magnetic material is masking this part of the $M_S(T)$ curve. In both $NRM(T)$ magnetization planes an additional slight decrease can be observed around 380°C that could be attributed to the maghemitized TM60 as a minor carrier of NRM. During cooling from 600°C, the $NRM(T)$ phase is randomly distributed. In this example, the remanence-carrying mineral can only be magnetite that was present either as a magmatic phase or as the result of titanomaghemite inversion under seafloor conditions.

The 102 Ma old sample 550B is characterized by a single maghemitized TM60 phase with $T_C = 295$°C (Fig. 1f). The absence of the maximum in $M_S(T)$ above room temperature is expected for a maghemitized TM 60 of this age (Matzka *et al.* 2003). Compared to samples 507B, 77B and 556, there is no significant temperature shift between $M_S(T)$ and $NRM(T)$, a fact that could be attributed to the high age of the sample leading to a similar, final degree of maghemitization for both the coarse and fine grained titanomaghemites. However, the NRM shows an unblocking spectrum that reaches to almost 400°C and the concave NRM decrease between 200°C and 400°C could be attributed to a grain size distribution that leads to a broad temperature spectrum where the single-domain to superparamagnetism transition occurs. The hysteresis parameters (Table 1) of sample 550B are compatible with such behaviour. During cooling, $NRM(T)$ shows a preferred orientation that is independent from the original NRM direction and likely is an artefact of the measurement.

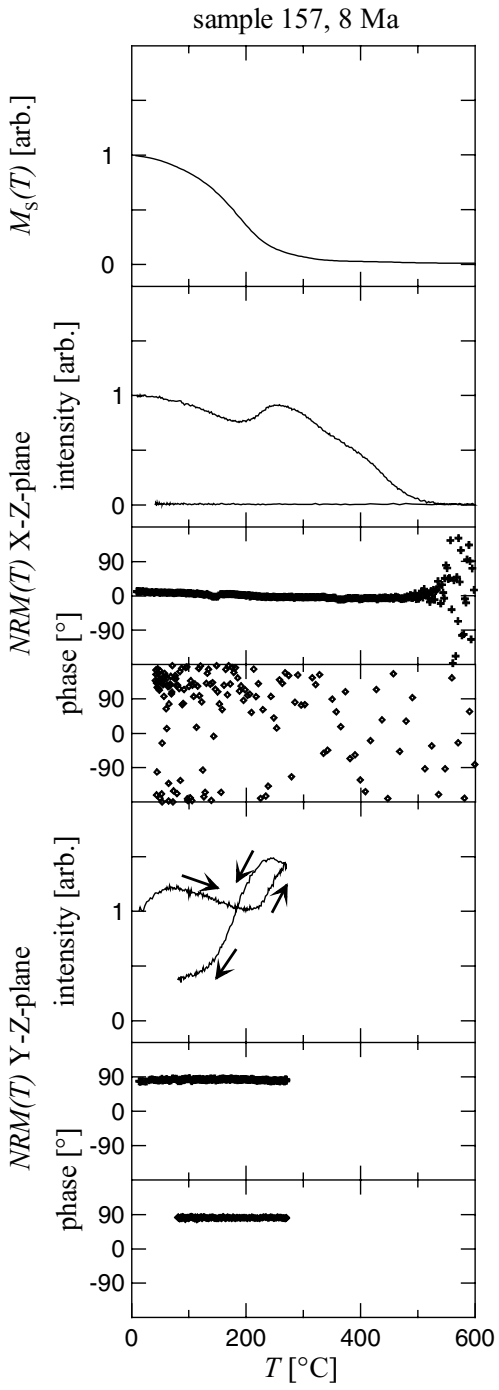

Figure 3. Comparison of strong field thermomagnetic curves $M_S(T)$ with continuous thermal demagnetization $NRM(T)$ for oceanic basalt sample 157 with self-reversal or partial self-reversal of NRM (*cf.* figure caption of Fig. 1).

Due to its very different behaviour, we discuss sample 157 last. Sample 157 is 8 Ma old and has a Curie temperature of 250°C (Table 1). The Curie temperature, age and absence of maximum in the $M_S(T)$ curve (upper panel of Fig. 3) above room temperature are compatible with a titanomaghemite with $x \approx 0.6$, $z \approx 0.5$, although a TM50 can not be excluded. For the CTD experiment in the X-Z plane, $NRM(T)$ intensity is decreasing between room temperature and 180°C and increasing again until 260°C before finally unblocking at 520°C. This suggests the presence of TM10 as remanence

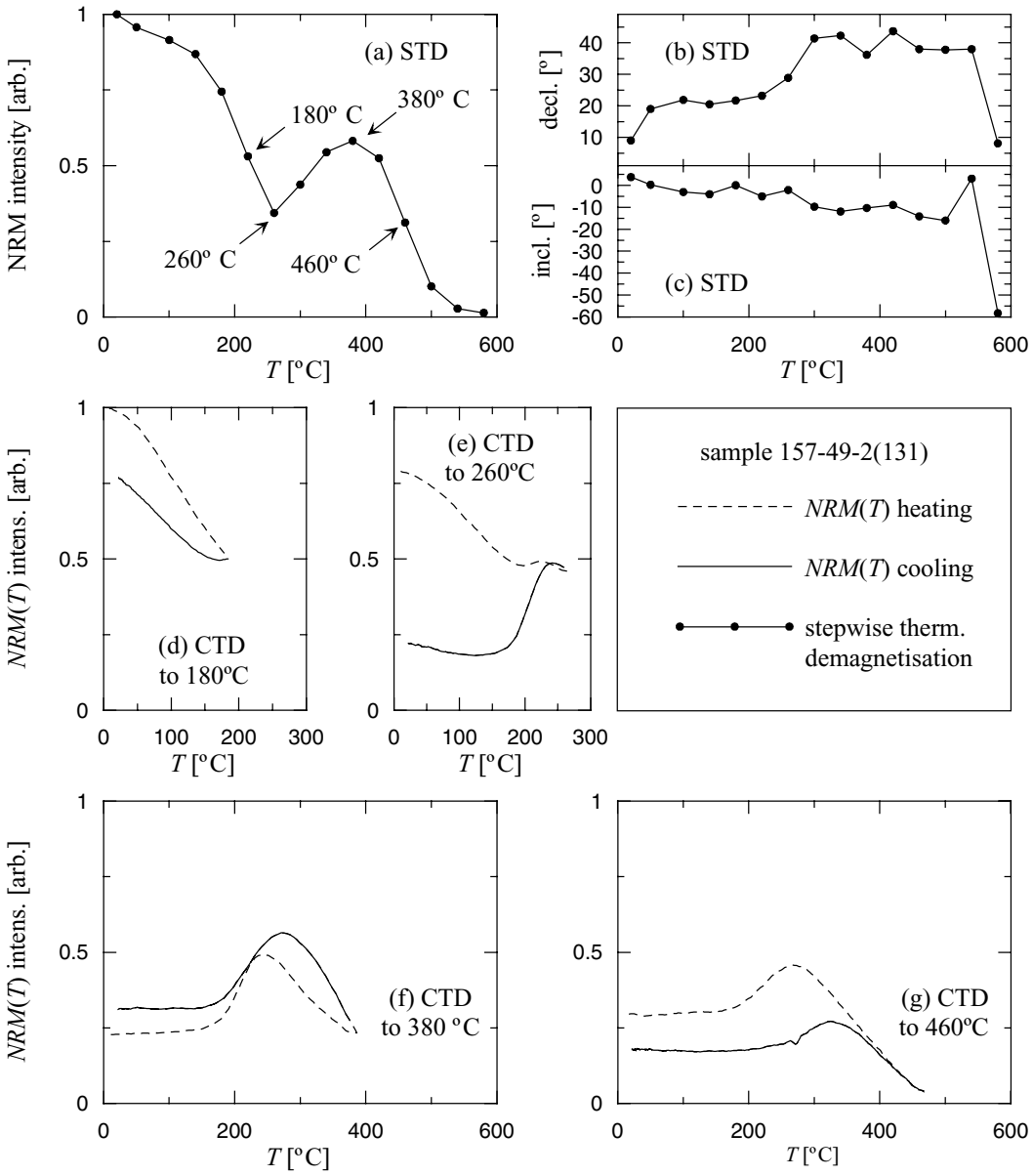

Figure 4. Stepwise (STD) and continuous (CTD) thermal demagnetization of sample 157 with self-reversal or partial self-reversal of NRM (*cf.* figure caption of Fig. 2).

carrier. The *NRM*(*T*) phase during heating is not as constant as for the other samples, but in first order the remanence direction remains stable. Consequently, the *NRM*(*T*) intensity in the *Y*-*Z* plane is not identical to the *X*-*Z* plane, but also has a minimum around 200°C. This heating run was stopped at 270°C, where *NRM*(*T*) is getting higher than at room temperature. Subsequent cooling leads to an overall decrease of *NRM*(*T*) intensity.

The STD experiment for sample 157 is shown in Figs 4(a)–(c). The inclination (in core coordinates) is shallow and changes progressively from 5° to −15°. Declination ranges from 10° to 40°, with the major change occurring synchronous with the increase in intensity after heating to 260°C. This increase leads to a maximum at 360°C. The remanence is finally demagnetized at 500°C to 540°C, at the same temperature where final unblocking was observed in the CTD experiment.

A sequence of CTD experiments to increasing maximum temperatures were measured for 157. *NRM*(*T*) to 180°C and back (Fig. 4d) already suggests that the irreversible NRM decrease of approximately 25% is occurring during cooling and that it is due to blocking of an antiparallel remanence. Such a behaviour can frequently occur in basalts (Krása *et al.,* 2005). This is confirmed by the next CTD experiment to 260°C in Fig. 4(e), where unblocking of the antiparallel remanence during heating and subsequently blocking of a much stronger antiparallel remanence during cooling is observed just below the maximum temperatures of 260°C. The intensity decrease in the STD between 140°C and 260°C (Fig. 4a) can clearly be attributed to the increasingly stronger antiparallel remanence, an effect which could be termed partial self-reversal during laboratory heating. Judging from the unblocking temperature of the antiparallel remanence, its remanence carrier must be the

titanomaghemite (or TM50) also observed in $M_S(T)$ in Fig. 3. During the subsequent CTD experiments to 380°C and 460°C in Figs 4(f) and (g) the blocking temperature of the antiparallel phase is increasing to approximately 280°C and 340°C, respectively, and the antiparallel blocked remanence is decreasing in intensity. The room temperature $NRM(T)$ intensity after the CTD experiments in Figs 4(d)–(g) correspond well to the intensities measured on the sister sample with the cryogenic magnetometer (Fig. 4a).

4 DISCUSSION

The usefulness of CTD data to better understand the sometimes complex behaviour of STD data of oceanic basalt NRM could be demonstrated for samples 556 and 157. CTD data also allows to clearly exclude certain magnetominerals for some samples (e.g. exclude magnetite as carrier of NRM in 556), but still has its limitations in unequivocally identifying the true remanence carrier. A limitation of the current setup of HOTSPIN I is the necessity for measurements of two subsamples in different planes to get the full vector information. Hence, the NRM properties of different subsamples have to be compared and might not necessarily reflect a homogenous magnetomineralogy. For example, the maximum in the NRM(T) heating curve at approximately 200°C for sample 556 is not identical in the *X*-*Z* plane and *Y*-*Z* plane in Fig. 1(d), but since there is hardly any change in remanence direction to be observed (crosses in Fig. 1d), the discrepancy is attributed to slight differences in the titanomaghemite composition (e.g. oxidation degree *z*). Inhomogeneity might also result from the distance to the pillow rim (Ryall & Ade-Hall 1975b) or from interstitial glass (Zhou *et al.* 2001). The same applies to the comparison of STD with CTD data.

The observation by Irving (1970) that STD unblocking temperatures of oceanic basalts by far exceed their Curie temperature is clearly confirmed by our best studied sample 556 (see Figs 1d and 2a). Despite the simple NRM-carrying phase (maghemitized TM60, Fig. 1d), the complex variation of NRM intensity during STD (Fig. 2a) looks similar to STD data of oceanic basalts showing partial self-reversal (Doubrovine & Tarduno 2004) or STD data with antiparallel overprint of the NRM (Wang *et al.* 2005). The reason for this is the thermal instability of the remanence carrier and a magnetic interaction of mother and daughter phase, conserving the original remanence direction. This process is also clearly observed in the $NRM(T)$ curves for sample 572D–34–1(99–101) and has been studied in detail, and linked to the inversion of titanomaghemite, by accompanying rock magnetic measurements (Krása & Matzka, 2007). The same applies to sample 77B, where CTD runs were performed to 480°C and 520°C (Fig. 1c) and the samples were still not fully demagnetized. The nature of the magnetic phase carrying the remaining remanence is unclear. A magnetite or a Ti-poor titanomagnetite formed during inversion of maghemitized TM60 and inheriting its remanence could provide the necessary chemical and magnetic stability at temperatures above 520°C (sample 77B) or 540°C (sample 556, STD in Fig. 2a). However, the $NRM(T)$ heating and cooling curves of 556 do not show a measurable remanence above 400°C (Figs 1d and 2g) and the shape of the cooling curve suggests that the magnetic remanence is only increasing when cooled below 400°C, corresponding to the final unblocking temperature observed in CTD. This could suggest, that the magnetite or Ti-poor titanomagnetite formed during inversion, that must geometrically be in close proximity to the original maghemitized TM60 to have inherited its remanence direction, is again giving its remanence direction to either a titanomagnetite with a blocking temperature around 400°C, or to remnants of the original maghemitized TM60. Again, the true nature of the magnetic phase in question could not unequivocally be established.

A rather common feature is that the parts of $NRM(T)$ curves associated with the magnetization decrease of maghemitized TM60 are shifted to approximately 80°C higher temperatures than the corresponding parts of the $M_S(T)$ curves, as seen for samples 507B, 77B and 556. This is the expected behaviour from a maghemitized TM60 phase that has a distribution of Curie temperatures where the smallest grains have highest oxidation degree and highest Curie temperature and are the most efficient remanence carrier (Bina & Prevot 1989). The temperature translates into a difference of mean oxidation parameter of $z \approx 0.25$. To our knowledge, the CTD data of 507B, 77B and 556 presents the first such evidence for grain-size-dependent alteration. A method similar to CTD, namely measuring small field (0.15 mT) thermomagnetic curves, was reported earlier by Johnson & Tivey (1995) for very young oceanic basalts (<20 ka) and later compared to strong field thermomagnetic curves (Kent & Gee 1996). However, detailed mineralogical analysis of the same rocks by Zhou *et al.* (1997) showed that these rocks contain an important range in titanium content of titanomagnetite ($0 < x < 0.8$) and that they might not be suitable to study grain-size-dependent alteration due to a lack of maghemitization. The 102 Ma old sample 550B might represent the state of a homogeneous, final oxidation degree of all grain sizes.

NRM unblocking temperatures of more than 500°C are observed even in CTD for samples 470A and 170. In both cases, a titanomagnetite (TM10 and TM00) is likely the carrier. The origin of these titanomagnetites and the process of remanence acquisition are unclear. Its origin could be magmatic, as observed by Zhou *et al.* 1997 (with a primary thermoremanence or TRM) or as titanomaghemite inversion product (either at seafloor conditions, as suggested in e.g. Kent & Gee (1994), or during laboratory heating) while inheriting the remanence from the mother phase. However, since the $NRM(T)$ intensity of sample 170 shows a rather constant decay between room temperature and unblocking, inversion during laboratory heating seems to be unlikely for this sample.

The presence of NRM-carrying titanomaghemite is also unclear in samples 470A and 170. At around 380°C sample 170 shows only a tiny, but systematic, decrease in $NRM(T)$. The unblocking temperatures of 470A between 300°C and 400°C would be compatible with maghemitized TM60, but the characteristic maximum in $NRM(T)$ above room temperature is missing. Therefore, this remanence might be carried by TM35, which would be untypical as inversion product of maghemitized TM60 (Özdemir 1987) and, therefore, likely is of magmatic origin (Zhou *et al.* 1997).

Sample 157 contains two remanence-carrying magnetic phases: TM10 and the titanomaghemite or TM50 phase, now referred to as low-T_C phase. We know from Figs 4(d)–(g) that these two phases are interacting and that they are negatively coupled in a way that the low-T_C phase gains a remanence antiparallel to the TM10 remanence on cooling through its blocking temperature. This behaviour results in a minimum in STD at 260°C and can be termed partial self-reversal during laboratory heating. Also, we know that the NRM of sample 157 in the thermally untreated state already is a composite of these two antiparallel remanences (Fig. 3). Therefore, the original NRM must be either self-reversed, or partially self-reversed. The remanence carried by TM10 is stronger than that of the low-T_C phase (Fig. 3). If the low-T_C phase is carrying the primary TRM, then sample 157 is carrying a self-reversed NRM. If the primary TRM is carried by TM10, then sample 157 has a partially self-reversed NRM. ODP site 157 was drilled on an equatorial site in the east

Pacific, and since the samples are azimuthally not oriented, no attempt has been made to use the NRM directional information to solve this question. One possible interpretation of the genetic relationship is that the original TM60 maghemitized and partially inverted to TM10 with antiparallel inheritance of the remanence. This would imply that inversion took place under seafloor conditions. In any case, the mechanism of self-reversal or partial self-reversal for oceanic basalt 157 is different to the process inferred by Doubrovine & Tarduno (2004) for oceanic basalts of high age and high maghemitization degree and probably rather resembles the mechanism proposed by Krása *et al.* (2005) for subaerial basalts.

5 CONCLUSIONS

By applying CTD and in two cases also STD to a suit of oceanic basalts with well-characterized rock magnetic properties (Table 1), the properties of their NRM were investigated with the aim to infer the magnetomineralogy of the NRM carrier. For some samples (507B, 77B and 556) the higher degree of maghemitization of the remanence-carrying titanomaghemite fraction (Bina and Prevot 1989) could be confirmed by CTD. In one sample, 157, a negative magnetic interaction between two remanence-carrying magnetomineralogical phases and a self-reversal or partial self-reversal of NRM was observed. Samples 157, 470A and 170 show a final unblocking of NRM above 500°C during CTD, indicating remanence carriers with a composition close to magnetite. The origin of this phase remains unclear and could vary from sample to sample. It could be magmatic or an inversion product of titanomaghemite either at seafloor conditions or during laboratory heating. Even oceanic basalts with rather simple magnetomineralogy containing only maghemitized TM60 as remanence carrier can have complex STD data.

ACKNOWLEDGMENTS

The authors would like to thank N. Petersen, H. Soffel, R. Leonhardt and C. Heunemann for helpful discussions. Rob Van der Voo and one anonymous reviewer are thanked for their constructive comments on the manuscript. Samples were provided by the Integrated Ocean Drilling Program (IODP). This research was funded by the Deutsche Forschungsgemeinschaft.

REFERENCES

Bina, M.M. & Prevot, M., 1989. Thermomagnetic investigations of titanomagnetite in submarine basalts: evidence for differential maghemitization, *Phys. Earth. Planet. Inter.,* **54**, 169–179.

Doubrovine, P.V. & Tarduno, J.A., 2004. Self-reversed magnetization carried by titanomaghemite in oceanic basalts, *Earth planet. Sci. Lett.,* **222**, 959–969.

Doubrovine, P.V. & Tarduno, J.A., 2005. On the compositional field of self-reversing titanomaghemite: constraints from the Deep Sea Drilling Project Site 307, *J. geophys. Res.,* **110**, B11104, doi:10.1029/2005JB003865.

Doubrovine, P.V. & Tarduno, J.A., 2006. N-type magnetism at cryogenic temperatures in oceanic basalt, *Phys. Earth planet. Inter.,* **157**, 46–54.

Dunlop, D.J. & Özdemir, Ö., 1997. *Rock Magnetism: Fundamentals and Frontiers*. 1st edn, p. 51, Cambridge University Press, Cambridge

Irving, E., 1970. The Mid-Atlantic Ridge at 45° N. XIV. Oxidation and magnetic properties of basalt; review and discussion, *Can. J. Earth. Sci.,* **7**, 1528–1538.

Johnson, H.P. & Tivey, M.A., 1995. Magnetic properties of zero-age oceanic crust; a new submarine lava flow on the Juan da Fuca Ridge, *Geophys. Res. Lett.,* **22**, 175–178.

Kent, D.V. & Gee, J., 1994. Grain size dependent alteration and the magnetization of oceanic basalts, *Science,* **265**, 1561–1563.

Kent, D.V. & Gee, J., 1996. Magnetic alteration of zero-age oceanic basalt, *Geology,* **24**, 703–706.

Krása, D. & Matzka, J., 2007. Inversion of titanomaghemite in oceanic basalt during heating, *Phys. Earth. Planet. Inter.,* **160**, 169–179.

Krása, D., Shcherbakov, V.P., Kunzmann, T. & Petersen, N., 2005. Self-reversal of remanent magnetization in basalts due to partially oxidized titanomagnetites, *Geophys. J.Int.,* **162**, 115–136.

Matzka, J., 2001. Besondere magnetische Eigenschaften der Ozeanbasalte im Altersbereich 10 bis 40 Ma. *PhD thesis*, Ludwig-Maximilians-Universität, Munich, http://edoc.ub.uni-muenchen.de/archive/00000428/01/Matzka˙Juergen.pdf

Matzka, J., Krása, D., Kunzmann, Th., Schult, A. & Petersen, N., 2003. Magnetic state of 10 to 40 Ma old ocean basalts and its implications for natural remanent magnetization, *Earth planet. Sci. Lett.,* **206**, 541–553

Özdemir, Ö., 1987. Inversion of titanomaghemites, *Phys. Earth planet. Inter.,* **46**, 184–196.

Petersen, N., 1976. Notes on the variation of magnetization within basalt lava flows and dikes, *Pageoph,* **114**, 177–193.

Petersen, N., Eisenach, P. & Bleil, U., 1979. Low temperature alteration of the magnetic minerals in ocean floor basalts, in *Deep Drilling Results in the Atlantic Ocean: Ocean Crust,* ed. Talwani M., *Maurice Ewing Series,* **2**, pp. 169–209, American Geophysical Union, Washington, DC.

Readman, P.W. & O'Reilly, W., 1972. Magnetic properties of oxidized (cation-deficient) titanomagnetites (Fe, Ti, □)$_3$O$_4$, *J. Geomagn. Geoelectr.,* **24**, 69–90.

Ryall, P.J.C. & Ade-Hall, J.M., 1975a. Laboratory induced self-reversal of thermoremanent magnetisation in pillow basalts, *Nature,* **257**, 117–118.

Ryall, P.J.C. & Ade-Hall, J.M., 1975b. Radial variation of magnetic properties in submarine pillow basalts, *Can. J. Earth. Sci.,* **12**, 1959–1975.

Wang, D., Van der Voo, R. & Peacor, D.R., 2005. Why is the remanent magnetic intensity of Cretaceous MORB so much higher than that of mid to late Cenozoic MORB? *Geosphere,* **1**, 138–146.

Zhou, W., Van der Voo, R. & Peacor, D.R., 1997. Single-domain and superparamagnetic titanomagnetite with variable Ti-content in young ocean-floor basalts: no evidence for rapid alteration, *Earth Planet. Science Lett.,* **150**, 353–362.

Zhou, W., Van der Voo, R. & Peacor, D.R., 1999. Preservation of pristine titanomagnetite in older ocean-floor basalts and its significance for paleointensity studies, *Geology,* **27**, 1043–1046.

Zhou, W., Van der Voo, R., Peacor, D.R., Wang, D., Zhang, Y., 2001. Low-temperature oxidation in MORB of titanomagnetite to titanomaghemite: a gradual process with implications for marine magnetic anomaly amplitudes, *J. geophys. Res.,* **106**, 6409–6421.